

## STATUS OF ELECTRON COOLING AT TARN II

*T.Tanabe, I.Katayama, N.Inoue, K.Chida, T.Watanabe, Y.Arakaki,  
K.Noda<sup>†</sup>, T.Honma<sup>‡</sup>, T.Shoji<sup>¶</sup>, and Y.Sakawa<sup>¶</sup>,*

Institute for Nuclear Study, University of Tokyo, Tanashi, Tokyo 188, Japan

<sup>†</sup> National Institute of Radiological Sciences, Chiba 260, Japan

<sup>‡</sup>Cyclotron and Radioisotope Center, Tohoku University, Sendai 980, Japan

<sup>¶</sup> Plasma Science Center, Nagoya University, Nagoya 464, Japan

### ABSTRACT

The electron cooler at TARNII has mainly been used for atomic and molecular physics experiments since 1991 when fundamental electron cooling tests finished. In this paper, some observed results during cooling and their analyses are reported.

### 1. INTRODUCTION

The TARNII is a storage ring [1] having a circumference of 78 m with electron cooler [2]. Light and heavy ions are injected from a sector focusing cyclotron with a K-number of 67. The first cooling experiments took place in September 1989. The electron cooler has recently been used mainly for the atomic and molecular physics experiments [3,4]. It is used to improve the momentum resolution and to reduce the transverse emittance of ion beams. It is also important for the stacking of low-intensity ion beams available from the cyclotron. The electrons of the cooler are a good electron target which can be adjusted to a finite velocity relative to the ion beams. Although time for studies of electron cooling has been quite limited, there has been some progress relating to the electron cooling technique.

For the parameters of the TARNII ring, the horizontal and vertical beta functions at the cooling section are 11 and 2.4 m, respectively. The dispersion function at the cooling section is as large as 4.9 m. Typical horizontal and vertical tune values during cooling are about 1.7 and 2.1, respectively. Average vacuum pressure is about  $1 \times 10^{-10}$  Torr. So far we stored molecular ion beams as well as atomic ion beams. They are p, d,  $^3\text{He}^+$ ,  $\text{He}^{++}$ ,  $\text{N}^{5+}$ ,  $\text{N}^{7+}$ ,  $\text{H}_2^+$ ,  $\text{H}_3^+$ ,  $\text{HD}_2^+$ ,  $\text{HeH}^+$ ,  $\text{HeD}^+$  and  $\text{CH}^+$ .

The electron cooler has a layout with vertical U-shape. The electron energy and current can be changed over a wide range. The cooling experiments, however, have been performed only at the injection energies. So, electron energies are typically less than 12 keV and currents are at most 1 A. Electron beam diameter is 50 mm.

This paper describes typical results obtained in recent cooling experiments and their analyses.

### 2. BEAM PROFILE MEASUREMENTS

An accurate alignment of the electron and ion-beam axes is essential for efficient electron cooling. The beam width in transverse direction is very sensitive to such alignment accuracy. In order to observe the horizontal beam profile without destructing the circulating ion beam, a residual gas ionization beam profile monitor was designed. The ion-electron pairs produced by the impact of the ion beam on residual gas are accelerated in the uniform electric field, and the residual gas ions bombard the surface of a micro-channel plate (MCP). MCP event location is determined by a resistive anode using charge division or risetime encoding technique [5,6]. One-dimensional projection of the beam profile can thus be obtained.

Fig. 1 is a photograph of the profile monitor. A Chevron type MCP with a sensitive area of 100 mm (transverse)  $\times$  15 mm (longitudinal) and one dimensional resistive anode are mounted together. The resistive anode comprises a sheet resistor with a total resistance of 250 k $\Omega$ . In order to identify the beam position, 4 parallel bars with a width of 1 mm are installed on the entrance of the MCP. A uniform electric field used to accelerate ionized residual gas was generated by applying a voltage of 10 kV between the upper and lower plates, which was divided by a resistor string and also applied to the intermediate electrodes. Since the electric field slightly steers circulating ion beams vertically, it is compensated by a reverse electric field formed by the same electrodes installed downstream of the profile monitor.

For position measurements, both charge-division and pulse-risetime methods have been tested. Although they gave almost the same position resolutions, the second method can work at higher count rates. Fig. 2 represents a measured beam profile of 85-MeV  $\text{N}^{5+}$  ions with and without electron cooling. The beam width changed from 60 mm (FWHM) to 1 mm with cooling. This means that the emittance was compressed from 90  $\pi$  mm mrad to 0.025  $\pi$  mm mrad after cooling. The profiler is used for the diagnostics of cooling like Schottky signal.

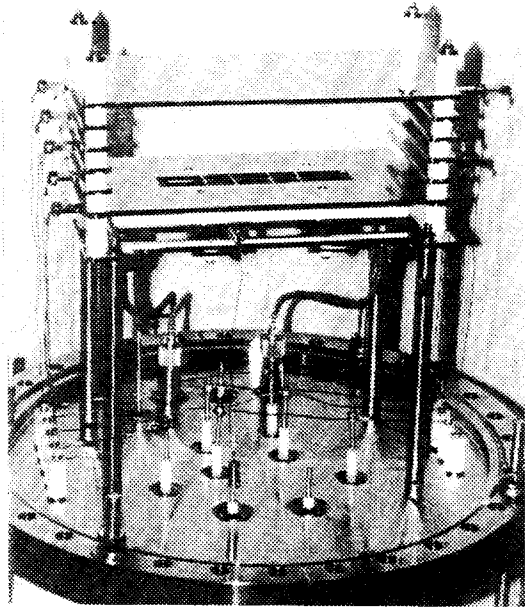


Fig. 1. Photograph of horizontal beam profile monitor.

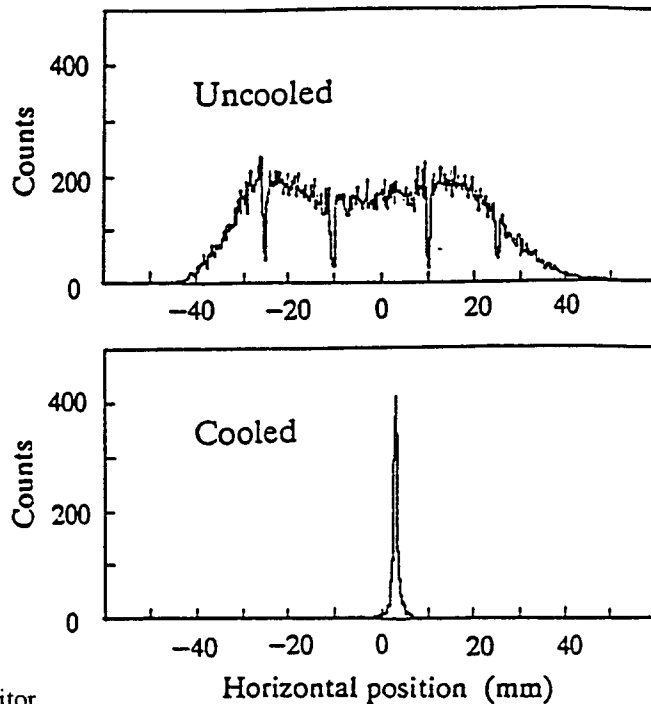


Fig. 2. Horizontal beam profiles for (a) uncooled and (b) cooled 85-MeV  $N^{5+}$  beams. The dips in the profile result from the shadows of 1-mm thick wires, which are inserted to calibrate the beam position.

### 3. BEAM STACKING

The beam intensity stored in the ring can be increased by the repeated multiturn injection with cooling, called "cool stacking". In this case, a part of the phase space volume prepared for the multiturn injection is occupied by the cooled and stacked beam. Fig. 3 shows an example of the cool stacking for 20-MeV proton beam, in which the beam was injected every 4 s and cooled. The intensity of the injected beam is about 10  $\mu\text{A}$  at a multiturn batch. The injection and cooling were repeated many times. After 50 injections in a time of 3 min, an intensity multiplication factor of about 30 was reached, resulting in the total number of stored particles of  $2.4 \times 10^9$ . The intensity saturates gradually due to finite beam lifetime, increasing beam size and so on. Sometimes we observed sudden loss of the beam, probably due to some instabilities.

### 4. SCHOTTKY SIGNAL MEASUREMENTS

The frequency spectra of the cold beam Schottky signals show splitting. The splitting becomes remarkable with the increase in number of circulating particles. It is originated from two plasma waves propagating parallel and antiparallel to the beam direction with a characteristic frequency  $f_c$  that is half the peak distance [7]. Fig. 4 shows the splitting of frequency spectrum of 61st harmonics of Schottky signal for 16-MeV proton beam with electron current of 0.4 A. The spectrum shows splitting even at a low current as 3  $\mu\text{A}$ . Estimated momentum resolution  $\Delta p/p$  (FWHM) is  $1.6 \times 10^{-5}$  and  $4.7 \times 10^{-5}$  at the currents of 7 and 90  $\mu\text{A}$ , respectively. The longitudinal coupling impedance ( $Z_n/n$ ), which can be deduced from  $f_c$  and number of circulating particles, is about 1.5  $\text{k}\Omega$ . Sometimes a triple-peak structure was observed, where the central peak position corresponded to the position of the harmonics of the revolution frequency. Self bunching of the beam (60  $\mu\text{A}$ ) was observed even when we switched off the RF voltage. The Schottky spectrum becomes more stable and sharper when we detuned the frequency of RF cavity from the revolution frequency. The improvement of the momentum resolution from our previous measurements [2] seems partly due to the reduction of ripple voltages of the high-voltage power supply which accelerates electrons. This power supply has a fast response time of 1 ms and can reduce the slow component of ripple voltages to a level to 0.1  $V_{p-p}$  which is low in comparison with our previous ripple level of 3  $V_{p-p}$ .

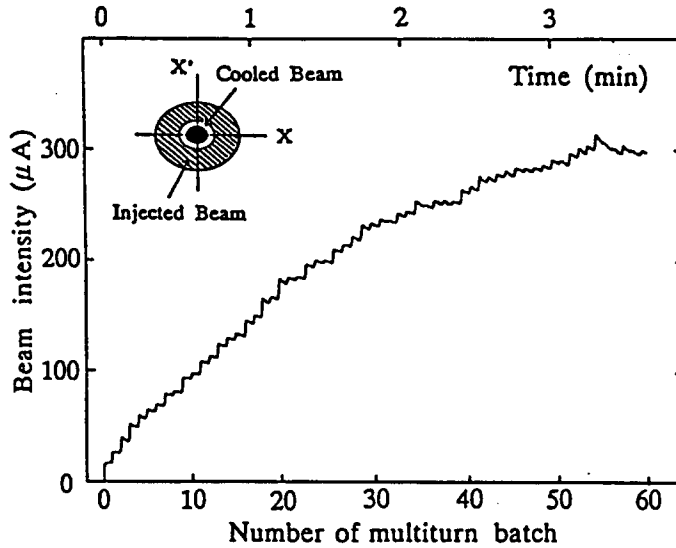


Fig. 3. Intensity increase during cool stacking as a function of the number of multiturn batches. The inset shows schematically represented phase spaces for the cooled and stacked beam and for the multiturn injected beam.

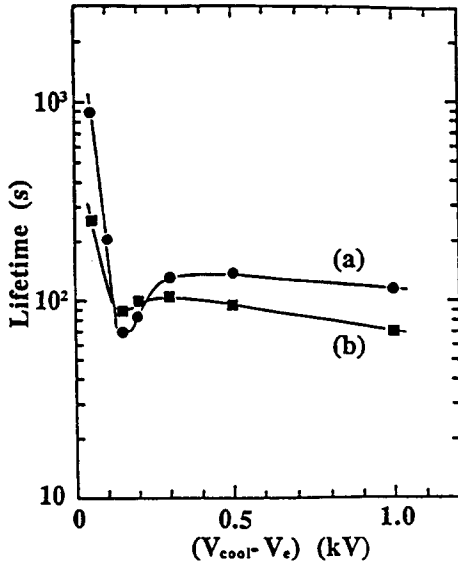


Fig. 5. Beam lifetime ( $1/e$ ) as a function of electron acceleration voltage for (a) coasting beam and (b) bunched beam (voltage:  $18 V_{p-p}$ ) measured with a DC current transformer. Beam is 20-MeV proton and its current is about  $40 \mu A$ . Tuned electron voltage ( $V_{cool}$ ) and current are 11.218 kV and 0.3 A, respectively.

### 5. EFFECTS OF DETUNED ELECTRON BEAM

An apparent beam loss in time of about 1 s after injection has been observed in a bunched beam cooling even with electron energy far detuned from the cooling energy. Such a decrease has been observed by using an electrostatic position monitor which is sensitive only to the bunched beam current. However, the current decrease, when measured with a DC-current transformer (DCCT) which was recently installed in the ring, was much slow. We try to understand the particle behavior when the electron velocity does not match the synchronous particle velocity. In order to find the electron cooling phenomenon easily, we used the small bucket with bucket height of  $20 V_{p-p}$  (for 20-MeV proton) which corresponds to the proton momentum width of  $\Delta p/p \sim 0.3 \times 10^{-3}$ . On the other hand, the initial uncooled proton momentum width is equal to about  $1 \times 10^{-3}$ . If the electron energy is tuned to the bucket center, the injected beam is cooled into the bucket center. This can be observed by the fast increase of the AC beam current with time in contrast to almost constant DCCT current. If we now detune the electron energy from the bucket center by an amount less than bucket height, a "ring" of beam is formed inside of the bucket [8].

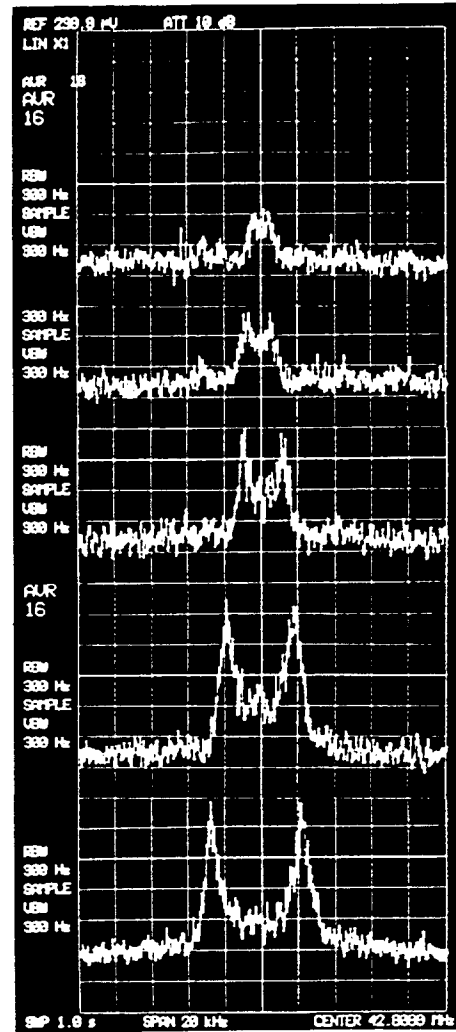


Fig. 4. Splitting of frequency spectrum of Schottky signal with increase in stored beam intensity (16-MeV p). From the top, intensities (number of particles) are 3  $\mu A$  ( $2.6 \times 10^7$ ), 7 ( $6.2 \times 10^7$ ), 16 ( $1.4 \times 10^8$ ), 54 ( $4.8 \times 10^8$ ) and 90 ( $8 \times 10^8$ ).

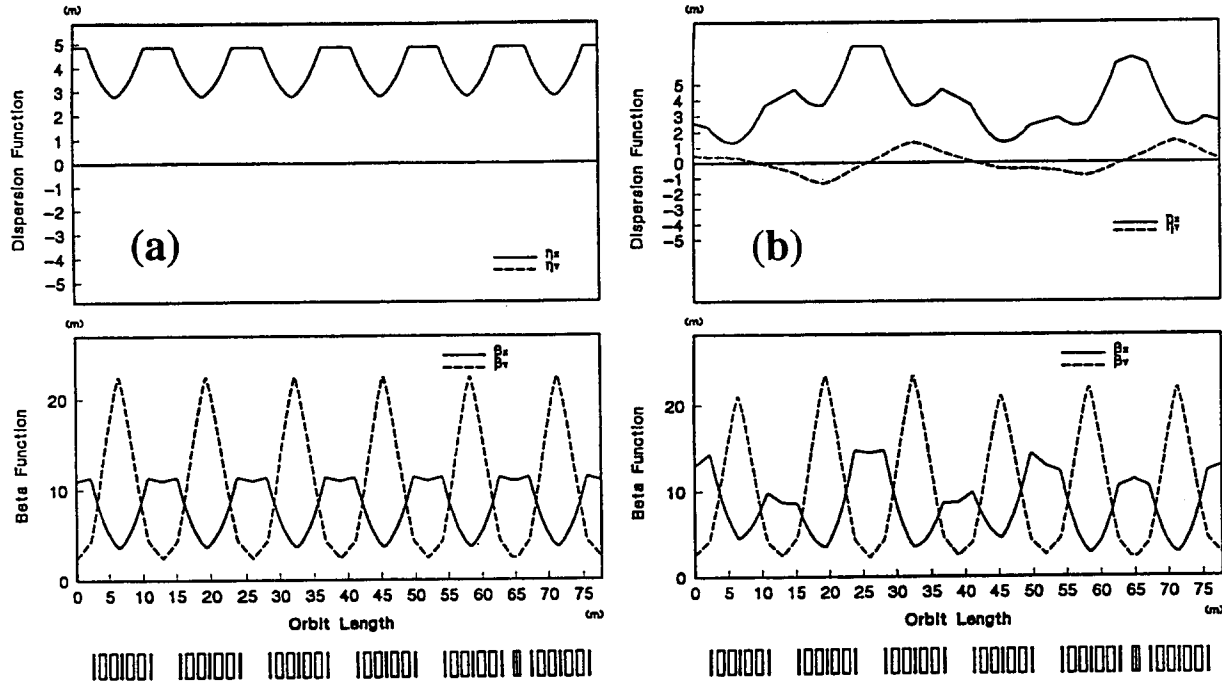


Fig. 6. Beta and dispersion functions (a) without electrons and solenoid field and (b) with an electron current of 4 A and a solenoid field of 0.6 kG. Electron cooler locates at the orbit length of about 65 m.

In this case, the AC and DCCT currents give almost the same results as the above ones. If we further detune the electron energy exceeding the bucket height, protons are siphoned out of the bucket, resulting in the fast decrease of the AC current after injection. The cooled DC component of the beam, however, still remains outside of the bucket, which gives slow decrease of the DCCT current. The experimental findings on the AC and DCCT currents behavior in case of the detuned electron energy can qualitatively be explained by such a consideration.

Fig. 5 shows the bunched and coasting beam lifetimes when the electron energy is shifted from the cooling energy. The lifetimes decrease rapidly and then get stabilized as the electron energies move apart from the tuning energy. There are minimums at around 0.15 kV. As the dispersion function at the cooling section is large, the beam moves horizontally by about the electron beam diameter of 50 mm if its energy is dragged to the one corresponding to the electron energy at the minimum. The dips seem to have a relation with such a beam movement. The coasting beam lifetime is generally longer than the bunched beam lifetime. The beam lifetimes at the far detuned electron energies are by about factor of 2-3 shorter in comparison with the ones without electron beam. The ion beam is affected by the electron beam despite negligibly small drag force at large detuning energies.

We try to understand such a phenomenon by taking account of the radial force due to the electron space charge. The radial electric field is linear inside the electron beam, while it changes as  $1/r$  outside the electron beam. So particles feel different forces inside and outside of the electron beam. If the ion beam comes out of the electron beam due to the misalignment of the beams or the larger beam size than the electron beam, a deformation of phase space area occupied by the beam may happen. In order to study the behavior of the beam under the detuned electron beam, we did simulations using a program in ref. [9], neglecting the drag force under following conditions,

initial tunes:  $Q_x=1.75$ ,  $Q_y=2.15$ , beta and dispersion functions at cooling section:  $\beta_x=11$  m,  $\beta_y=2.4$  m,  $\eta_x=4.9$  m, electron-diameter: 50 mm, -length: 1 m, solenoid field: 0.6 kG (uncompensated), initial beam (20-MeV proton) at cooling section:  $|x| \leq 40$  mm,  $|x'| \leq 3.7$  mrad,  $|y| \leq 10$  mm,  $|y'| \leq 4.5$  mrad.

In the calculations, the magnetic field produced by the electron beam was neglected as its effect is small. Fig. 6 shows the differences of beta and dispersion functions with and without electrons and solenoid field which were calculated taking account of the linear part of the space-charge force. As can be seen in the figure, they change much and the vertical dispersion ( $\eta_y$ ) newly appears due to the solenoid field. Tune shifts are  $\Delta Q_x=+0.044$  and  $\Delta Q_y=+0.009$  which are mainly due to the electron current of 4 A. Fig. 7 shows phase plots for particles with a momentum larger than the central particles by  $\Delta p/p=+0.2\%$  at  $I_e=0, 1$  A and 4 A, including linear and non-linear space-charge forces. Particle phases are plotted every  $10^3$  turns up to  $10^4$  turns altogether on the horizontal and vertical phase spaces. As can be seen in the figure, the separatrix becomes unclear and the beam size expands with

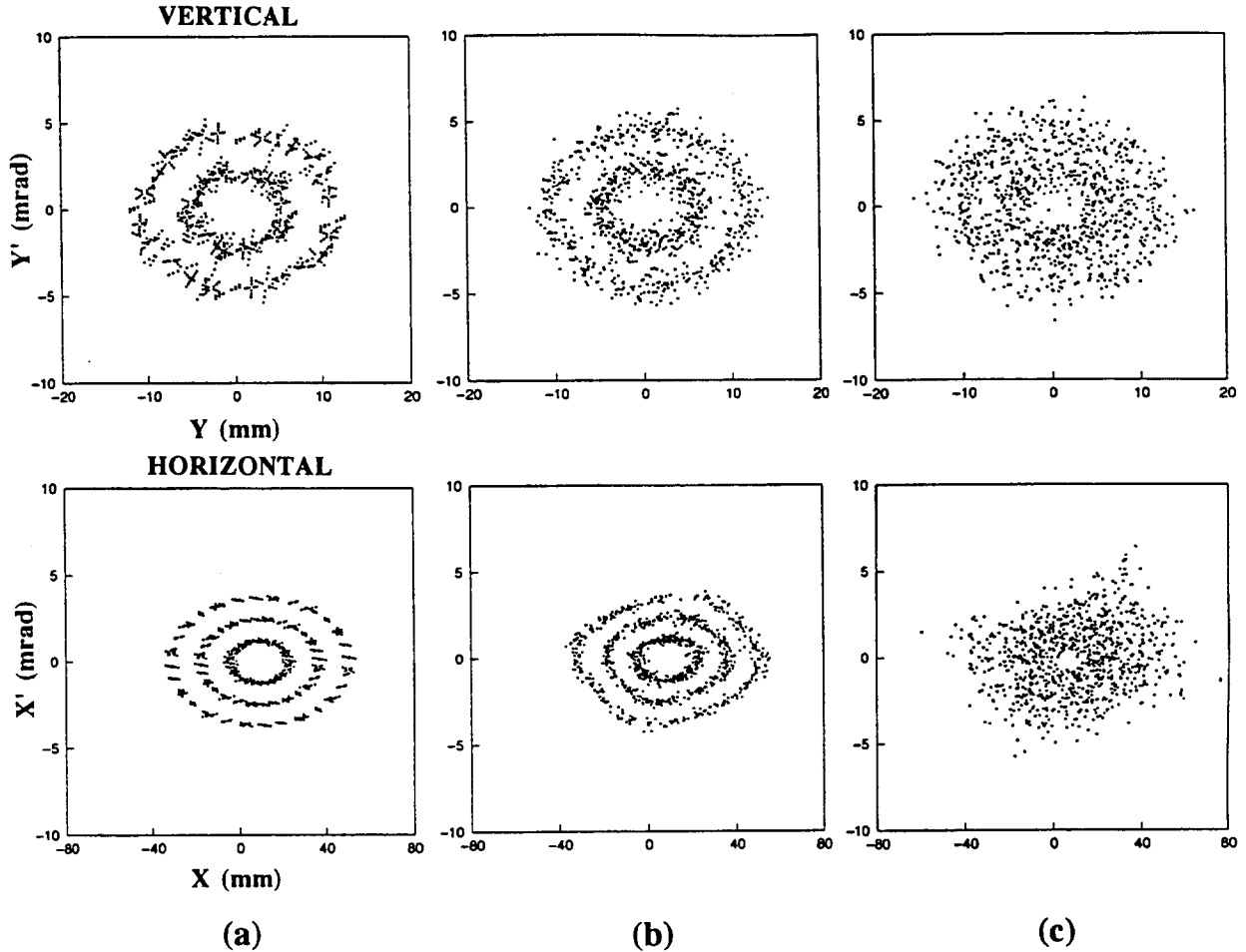


Fig. 7. Phase plots of 20-MeV protons with a momentum deviation of  $\Delta p/p = +0.2\%$  for the electron currents of (a) 0 A, (b) 1 A and (c) 4 A.

the increase of electron current. This tendency is especially remarkable for the particles outside of the electron beam and those having large momentum deviation. The plots are only  $10^4$  turns which correspond to 14 ms. So the beam quality becomes much worse in the time of the order of seconds. From these simulation studies, it can be concluded that followings are important in order to avoid the beam loss: 1) overlap of electron and ion beams, 2) compensation of solenoid field, 3) zero dispersion at the cooling section and 4) small beta functions. Although this phenomenon is not serious for our ring practically, the simulated results seem to suggest the origin of strong "electron heating" observed at CELSIUS [10].

## REFERENCES

- [1] T. Katayama et al., *Present status of cooler synchrotron TARNII*, Proc. of 7th Symposium on Accelerator Science and Technology, Osaka, pp. 35-37, (1989).
- [2] T. Tanabe et al., *Electron cooling experiments at INS*, Nucl. Instrum. Methods, A307, pp. 7-25, (1991).
- [3] T. Tanabe et al., *Dielectronic recombination of He<sup>+</sup> in a storage ring*, Phys. Rev. A45, pp. 276-280, (1992).
- [4] T. Tanabe et al., *Dissociative recombination of HeH<sup>+</sup> at large center-of-mass energies*, Phys. Rev. Lett. 70, pp. 422-425, (1993).
- [5] B. Hochadel, *Ein strahlprofilmonitor nach der methode der restgasionisation für den Heidelberger testspeicherring TSR*, MPI H-1990-V-19, (1990).
- [6] J.L. Wiza, *Microchannel plate detectors*, Nucl. Instrum. Methods 162, pp. 587-601 (1979).
- [7] H. Poth et al., *First results of electron cooling experiments at LEAR*, Z. Phys. A332, pp. 171-188, (1989).
- [8] W. Kells and F. Mills, *Dynamics of R.F. captured electron cooled proton beams*, Fermilab TM-1153 (1983).
- [9] K. Noda et al., *A use of a thin foil target in a cooler ring experiment*, Nucl. Instrum. Methods, A303, pp. 215-225, (1991).
- [10] D. Reistad et al., *Recent commissioning results at CELSIUS*, Proc. of 13th Int. Conf. Cyclotrons and Their Applications, Vancouver, pp. 266-273, (1992).